Kinetic analysis of immunocomplexation with photoimmobilized F(ab')$_2$ on planar optical waveguides

H. GAO, H. SIGRIST
Institute of Biochemistry, University of Bern, Freiestrasse 3, CH-3012 Bern, Switzerland

Immunocomplexation at waveguiding TiO_2/SiO_2 surfaces was monitored with an integrated optical grating coupler, and the kinetic parameters of antigen binding to surface-immobilized F(ab')$_2$ fragments of a monoclonal antibody were determined. Ternary immunocomplexes were formed with photoimmobilized F(ab')$_2$ fragments, the prostate specific antigen (PSA) and a second monoclonal antibody which recognizes a different epitope on PSA. The kinetic analyses of antibody–antigen interaction revealed a high antigen affinity for the surface-immobilized first antibody. The second antibody, applied in solution, showed low affinity to PSA. The correlation between immunocomplex formation and the antigen concentration was linear in the range of 2 to 50 nM (correlation coefficient 0.973). Kinetic analyses were also carried out with regenerated immunosensors, reversible regeneration of immunocompetent surfaces being attained by treatment with 0.1 M glycine, pH 2.3. The coefficient of variation of the kinetic parameters was 5.5% to 8.2% with five repeats.

1. Introduction

Biosensors provide analytical tools for the elucidation of molecular interactions [1]. Evanescent optical sensing techniques which detect adlayer changes close to or at surfaces, are finding increased application in real-time analysis of molecular binding events. Integrated optic techniques register refractive index changes and allow on-line registration of formed adlayer thickness [2]. The techniques mentioned are of particular interest since labelling of bioanalytes is not required. To date, instrumentation based on surface plasmon resonance or on waveguiding principles is available, allowing the detection of molecular adlayers on sensor surfaces under carefully controlled and reproducible conditions [3, 4]. In current sensor technology, low-level (or reproducible) non-specific binding and cyclic regeneration of biocompetent surfaces are among the investigated topics. Repeat analysis with a single sensor device presupposes irreversible adherence or covalent immobilization of those molecules which take part in biological recognition. Characterization of the kinetics and thermodynamics of macromolecular interactions with biosensor techniques thus contributes to the understanding of the molecular basis of biological recognition.

The solid phase immunoassay technique is a convenient way to explore molecular interactions between antigens and antibodies. Biospecific binding is enabled by the molecular selectivity of the analyte for immobilized immunoreagents. Recently, versatile photolinker polymer-mediated biomolecule immobilization procedures have been described. Immobilized biomolecules retain their biospecificity on various materials and non-specific binding is suppressed [5, 6]. Assessment of kinetic parameters with solid phase assay systems has previously been reported. Determination of rate and equilibrium binding constants for macromolecular interactions using surface plasmon resonance was described by O'Shannessy and Pellequer [7, 8]. Sadana and collaborators investigated the kinetics of antigen binding to immobilized antibodies on fibre-optic surfaces [9, 10]. This work describes the kinetic analysis of immunocomplexation on planar optical waveguides, ternary immunocomplexes being formed with a photoimmobilized monoclonal antibody (pi-Ab_1F(ab')$_2$ fragment), a protein antigen (prostate specific antigen PSA) and a second monoclonal antibody (Ab_2) which recognizes a different epitope on PSA.

2. Materials and methods

Monoclonal anti-PSA antibodies (F5, 1A5-6) were obtained from Hoffmann-La Roche. Prostate specific antigen (PSA) was purchased from Milan Analytical AG. The photolinker polymer T-BSA (bovine serum albumin derivatized with 3-(trifluoromethyl)-3-(m-isothiocyano-phenyl) diazirine) was prepared according to published procedures [6]. Planar optical waveguides incorporating a grating coupler with a diffraction grating (period $1/\Lambda = 1200\ mm^{-1}$) were used (type 1400; 170–200 nm TiO_2/SiO_2 waveguiding layer on Corning glass). Photoimmobilization onto TiO_2/SiO_2 waveguiding layers was carried out as detailed

0957 4530

in reference [11] and immunocomplexation was analysed with the integrated optical sensor IOS-1 (Artificial Sensing Instruments, Zürich, Switzerland), equipped with a computer-controlled solvent delivery system (Universal, valve switching module). A peristaltic pump (Minipuls 3, Gilson) was used to expel all reagents through the flow cell and data were processed with the system software (version 2.4). After photoimmobilization, $F(ab')_2$ fragments of monoclonal anti-PSA modified sensor chips were stored at least overnight at 4 °C in buffer A (5 mM Tris, 10 mM NaCl, pH 7.4) containing 0.5% BSA. Chips were rinsed with water and placed in the chip holder of the grating coupler instrument. Routinely, sensor chips were pretreated with glycine buffer (0.1 M glycine; 0.5 M NaCl, pH 2.3) for 10 min to remove adsorbed BSA before measurements were started. The grating coupler immunosensor registers the formation of an adlayer F of thickness d_F on the T-BSA/$F(ab')_2$ co-polymer matrix. Upon immunoreagent binding, the effective refractive index change is $\Delta N_{eff} = (\delta N/\delta d_F)d_F$. The ΔN_{eff} due to antigen and 1A5-6 antibody binding can thus be monitored by measuring the incoupling angle. From these data the apparent waveguide thickness t_F (onward referred to as observed signal S) is calculated by the IOS-1 system software [12]. Repetitive antigen and 1A5-6 antibody binding to a sensor surface with photoimmobilized anti-PSA$F(ab')_2$ was attained with the following programmed sequence of solvent delivery: (i) regeneration with glycine buffer (0.1 M glycine, 0.5 M NaCl, pH 2.3); (ii) buffer A (10 mM Tris, 50 mM NaCl, pH 7.4); (iii) PSA (or PSA/anti-PSA 1A5-6 premixed in a 1:5 molar ratio); (iv) buffer A. On-line recorded data sets were generated with 2 to 50 nM ligand concentration, linearly transformed and processed with commercial fitting programmes.

3. Results and discussion

Experimental data were analysed according to integrated rate equations which describe the binding of soluble ligands to photoimmobilized macromolecules and the dissociation of formed complexes from the surface, respectively. Since the IOS-1 instrument is a continuous, real-time detector, reversible interactions can be assessed and the association (k_a) and dissociation (k_d) rate constants can be determined. The sandwich-type immunoassay includes three surface-associated reaction equilibria.

$$\text{pi-Ab}_1 + \text{Ag} \Leftrightarrow \text{pi-Ab}_1\text{Ag} \quad (1)$$

$$\text{pi-Ab}_1\text{Ag} + \text{Ab}_2 \Leftrightarrow \text{pi-Ab}_1\text{AgAb}_2 \quad (2)$$

$$\text{pi-Ab}_1 + \text{AgAb}_2 \Leftrightarrow \text{pi-Ab}_1\text{AgAb}_2 \quad (3)$$

3.1. Antigen binding to, and dissociation from, the photoimmobilized antibody

The rate of [pi-Ab_1Ag] binary immunocomplex formation at time t is

$$d[\text{pi-Ab}_1\text{Ag}]/dt = k_{a1}[\text{pi-Ab}_1][\text{Ag}] - k_{d1}[\text{pi-Ab}_1\text{Ag}] \quad (4)$$

where k_a is the association rate constant and k_d is the dissociation rate constant. The apparent concentration of photoimmobilized antibody on the surface at the reaction time t is

$$[\text{pi-Ab}_1] = ([\text{pi-Ab}_1]_0 - [(\text{pi-Ab}_1\text{Ag})] \quad (5)$$

Substituting the rate equation 4 gives

$$d[\text{pi-Ab}_1\text{Ag}]/dt = k_{a1}[\text{pi-Ab}_1]_0[\text{Ag}] - (k_{a1}[\text{Ag}] + k_{d1})[\text{pi-Ab}_1\text{Ag}] \quad (6)$$

The observed signal S is proportional to the formation of [pi-Ab_1Ag] (or [pi-Ab_1AgAb_2]) at the surface and the maximum signal (S_{max}) is proportional to the surface concentration of the immunoreactive photoimmobilized antibody (pi-Ab_1). The association rate equation of antigen binding to the immobilized antibody is therefore

$$dS_1/dt = k_{a1}[\text{Ag}]S_{max1} - (k_{a1}[\text{Ag}] + k_{d1})S_1 \quad (7)$$

Standard analysis of binding data recorded with the IOS-1 instrument allows the determination of k_0 (k observed) by plotting dS_1/dt versus S_1, k_0 is defined as

$$k_{01} = k_{a1}[\text{Ag}] + k_{d1} \quad (8)$$

Determination of k_0 with different antigen concentrations and plotting k_{01} versus [Ag] yields the association rate constants k_{a1} (slope) and the dissociation rate constant k_{d1} (y-intercept) of the immunoreaction. However, linear transforms also transform experimental errors. It is therefore advantageous to analyse the data directly in terms of the integrated form of the rate equation [7].

$$S_1 = k_{a1}[\text{Ag}]S_{max1}[1 - e^{-(k_0 t)}]/k_0 \quad (9)$$

In this equation the baseline response S_0 is set to zero although the instrument's baseline prior to antigen addition is not zero. Baseline correction of the experimental data can be achieved by subtracting S_0 before antigen admission. An alternative approach to baseline correction is described in Equation 10:

$$S_1 = k_{a1}[\text{Ag}]S_{max1}[1 - e^{-(k_0 t)}]/k_0 + S_{01} \quad (10)$$

where S_{01} is a system parameter equivalent to the signal at the time of antigen application ($t = 0$).

A simplified version of Equation 10 is obtained by substituting the term of the amplitude with the parameter A. A affects the amplitude of the exponential curve and can be used as fitting parameter.

$$S_1 = A_1[1 - e^{-(k_{01} t)}] + S_{01} \quad (11)$$

Antigen dissociation can be observed directly once the antigen solution has traversed the flow cell and the system reverts to buffer flow (Fig. 1a). The rate of surface linked immunocomplex dissociation is

$$dS_1/dt = -k_{d1}S_1 \quad (12)$$

The integrated rate equation was used to analyse the experimental data.

$$S_1 = S_{a1}\, e^{-k_{d1} t} \quad (13)$$

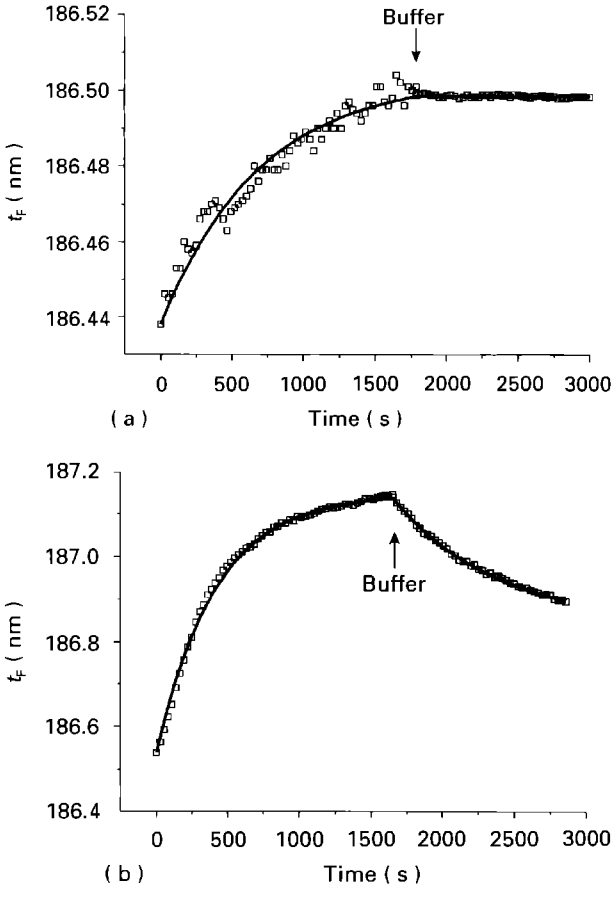

Figure 1 Binding of the antigen PSA and the second anti-PSA antibody (1A5-6) to the waveguide surface previously modified with F5 anti-PSA F(ab')$_2$ fragments. Experimental data (□) and best fit analysis (——) according to Equations 11 and 14 are shown for the association to, and dissociation of, PSA from photoimmobilized F(ab')$_2$ fragments (a) and the binding (Equation 16) and dissociation (Equation 18) of the second anti-PSA antibody (b). PSA 10 nM; association fitting, $\chi^2 = 1.3031 \times 10^{-5}$; A_1 0.065442; C 10^{-8}; K_{a1} 144296; K_{d1} 10^{-7}, Y_0 186.438. Dissociation fitting; $\chi^2 = 9.1571 \times 10^{-6}$; S_{a1} 0.0608297; K_{d1} 10^{-7}, Y_0 186.438. Anti-PSA (1A5-6), 50 nM; association fitting; $\chi^2 = 9.906 \times 10^{-5}$ A 0.609607; C; 5×10^{-8}; K_{a2} 21403; K_{d2} 0.00136544; Y_0 186.54. Dissociation fitting, $\chi^2 = 1.1042 \times 10^{-5}$; S_{a2} 0.407133; K_{d2} 0.00137; S_{a3} 0.294811; K_{d3} 0.00064 Y_0 186.438.

S_{a1} is the amplitude at the beginning of the dissociation process (reaction equilibrium 1) which is not known but can be used as a parameter for curve fitting. To account for the fact that even after complete dissociation of the immunocomplex from the surface of the sensor chip, the instrument response is not zero, the dissociation equation can be written as

$$S_1 = S_{a1}\, e^{-k_{d1} t} + S_{t\to\infty} \qquad (14)$$

where $S_{t\to\infty}$ is the response value after infinite time, implying complete dissociation of the immunocomplexes.

The above-mentioned equations were used to determine the kinetic constants k_{a3} and k_{d3} of the reaction equilibrium 3.

3.2. Binding and dissociation of the second antibody to anti-PSA/PSA immunocomplexes

The affinity of the second antibody to PSA was measured by binding the second antibody to preformed

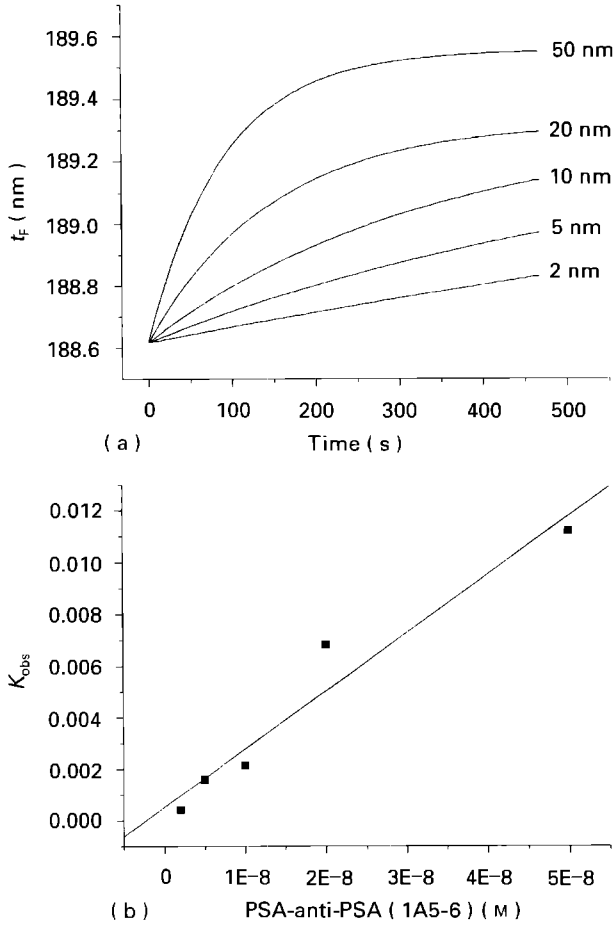

Figure 2 Formation of a ternary immunocomplex consisting of the photoimmobilized anti-PSA F(ab')$_2$ fragments (F5), PSA and the second anti-PSA antibody (1A5-6) which recognizes a different epitope of the antigen. Experimental data of PSA/anti-PSA 1A5-6 binding to photoimmobilized F(ab')$_2$ fragments were fitted according to Equation 11. The association and dissociation rate constants were determined by plotting k_0 versus the respective PSA/anti-PSA concentration according to Equation 8. Correlation; linear regression, $\chi^2 = 1.4461 \times 10^{-6}$; K_{a3} 225028.72432; $R = 0.97287$, SD = 0.0012, $N = 5$; K_{d3} 0.00052.

TABLE I Summary of the kinetic parameters describing the formation of a ternary immunocomplex on an immunosensor surface. F(ab')$_2$ fragments were photoimmobilized on the grating coupler sensor chip as described in the materials and methods section. The kinetic constants k_a were calculated according to Equations 11 and 16, k_d values were obtained applying Equations 14 and 18. The equilibrium constant of the reaction was calculated according to Equation 19.

Molecular interaction	k_a ($M^{-1} s^{-1}$)	k_d (s^{-1})	k_{eq} (M^{-1})
pi-F5/PSA	1.4×10^5	1.0×10^{-7}	1.4×10^{12}
pi-F5-PSA/1A5-6	2.1×10^4	1.4×10^{-3}	1.5×10^7
pi-F5/PSA-1A5-6	2.3×10^5	5.2×10^{-4}	4.3×10^8

[pi-Ab$_1$Ag] complexes (Fig. 1b). The association rate of this reaction is

$$dS_2/dt = k_{a2}[Ab_2]\, S_{max2} - (k_{a2}[Ab_2] + k_{d2})S_2 \qquad (15)$$

and integration of Equation 15 gives

$$S_2 = A_2[1 - e^{-(k_{02} t)}] + S_{02} \qquad (16)$$

TABLE II Kinetic characterization of the cyclic regenerated immunosensor surface. Repetitive binding of 10 nM preformed PSA/anti-PSA (1A5-6) binary complexes to surface-linked (photoimmobilized) $F(ab')_2$ was measured with the IOS-1 instrument. After incubation with PSA/anti-PSA (1A5-6) for 30 min, the chip was washed with buffer and regenerated by treatment with 0.1 M glycine, 0.5 M NaCl, pH 2.3. Five regeneration cycles were carried out and the kinetic constants were determined (Equations 11 and 14).

Cycle no.	A	k_{obs}	S	k_d (s^{-1})	k_a ($M^{-1}\,s^{-1}$)
n_1	0.5531	0.00304	0.6721	0.0006	2.40×10^5
n_2	0.6143	0.00297	0.7126	0.0006	2.39×10^5
n_3	0.5751	0.00276	0.6886	0.0007	2.06×10^5
n_4	0.5978	0.00262	0.7288	0.0006	2.02×10^5
n_5	0.5181	0.00255	0.6116	0.0007	1.85×10^5
$n \pm \sigma$ (%)	0.5716 ± 5.9	0.00279 ± 7.2	0.6712 ± 5.5	0.00064 ± 6.3	$2.21 \times 10^5 \pm 8.2$

Since the dissociation of [pi-Ab_1AgAb_2] may occur along two pathways, the dissociation rate equals

$$dS/dt = -(S_2 k_{d2} + S_3 k_{d3}) \quad (17)$$

k_{d3} was determined by binding to, and dissociation of [$AgAb_2$] from the surface. Integration of Equation 17 gives the fitting function

$$S_2 = S_{a2}\, e^{-(k_{d2} t)} + S_{a3}\, e^{-(k_{d3} t)} + S_{t \to \infty} \quad (18)$$

which was used to determine k_{d2}.

Equilibrium constants were calculated according to Equation 19:

$$K_{eq} = k_a/k_d \quad (19)$$

Sandwich-type immunocomplexes were formed on waveguide surfaces after photoimmobilization of anti-PSA $F(ab')_2$ fragments (pi-Ab_1). Fig. 1 shows the experimental data (open squares) and best fit analysis (full line) for the binding and dissociation of the antigen PSA (Fig. 1a). Fig. 1b depicts the association and dissociation of sandwich-type immunocomplexes after addition of the second antibody (1A5-6). k_a and k_d values were determined according to Equations 11 and 16, and 14 and 18, respectively.

Data reported in Fig. 2 demonstrate that the rate of the ternary immunocomplex formation on the photoimmobilized immunoreagents linearly correlates with the concentration of applied PSA/anti-PSA complexes (2 to 50 nM). Fitted binding curves are depicted in Fig. 2a. Observed rate constants k_0 were calculated according Equation 11 and plotted versus the respective analyte concentration ($AgAb_2$). Linear regression of the data set yielded the association rate constant $k_{a3} = 2.2 \times 10^5\ M^{-1} s^{-1}$ and a dissociation rate constant k_{d3} of $5.2 \times 10^{-4}\ s^{-1}$. Kinetic constants applying to the formation and dissociation of the pi-anti-PSA/PSA/anti-PSA ternary immunocomplex are summarized in Table I. The overall analysis of antigen–antibody interaction revealed a high antigen affinity for the surface immobilized first antibody. The second antibody applied in solution showed low affinity to PSA. The results agree with observations obtained by ELISA procedures.

Repetitive immunocomplex formation after glycine buffer treatment was investigated by determination of the kinetic parameters after each regeneration cycle. Table II lists the kinetic parameters and coefficients of variation from five repeats. The results indicate an overall 16% decrease of k_{obs} after the five cyclic regenerations.

Acknowledgements

Financial support from the Kommission zur Förderung der wissenschaftlichen Forschung, Bern (EUREKA project 2690.1) and the Swiss Priority Program on Biotechnology is acknowledged.

References

1. H. L. SCHMIDT, W. SCHUHMANN, F. W. SCHELLER and F. SCHUBERT, in "Sensors, a comprehensive study", edited by W. Goepel, J. Hesse and J. N. Zemel (VCH Verlagsgesellschaft, Weinheim, 1992) Vol. 3, Part II, p. 19.
2. W. HUBER, CH. BARNER, J. FATTINGER, H. HÜBSCHER, F. KOLLER, F. MÜLLER, D. SCHLATTER and W. LUKOSZ, *Sensors and Actuators B* **6** (1992) 122.
3. J. HODGSON, *Bio/Technology* **12** (1994) 31.
4. U. JÖNSSON, L. FÄGERSTAM, B. IVARSSON, B. JOHNSSON, R. KARLSSON, K. LUNDH, S. LÖFÅS, B.PERSSON and H. ROOS, *Bio/Techniques* **11** (1991) 620.
5. H. SIGRIST, H. GAO and B. WEGMÜLLER, *Bio/Technology* **10** (1992) 1026.
6. H. GAO, E. KISLIG, N. ORANTH and H. SIGRIST, *Biotechnol. Appl Biochem.* **20** (1994) 251.
7. D. J. O'SHANNESSY, M. BRIGHAM-BURKE, K. K. SONESON, P. HENSLEY and I. BROOKS, *Anal. Biochem.* **212** (1993) 457.
8. J. L. PELLEQUER and M. H. V. REGENMORTEL, *J. Immunol. Methods* **166** (1993) 133.
9. A. SADANA and D. SII, *Biosensors & Bioelectronics* **7** (1992) 559.
10. A. SADANA and A. M. BEELARAM, *ibid.* **10** (1995) 301.
11. H. GAO, M. SÄNGER, R. LUGINBÜHL and H. SIGRIST, *ibid.* **10** (1995) 317.
12. W. LUKOSZ and K. TIEFENTHALER, *Sensors and Actuators* **15** (1988) 273.

Received 29 June
and accepted 4 July 1995